

## EXPERIMENTAL EVIDENCE OF BULK HELICON-PHONON COUPLING IN PbTe

W. Schilz

Philips Zentrallaboratorium GmbH, Hamburg-Stellingen, Germany

(Received 20 November 1967)

In this Letter we present what we believe to be the first conclusive demonstration of helicon-phonon coupling in a semiconductor for both longitudinal and transverse acoustic waves. The experiments were carried out in PbTe single crystals at  $T = 4.2^\circ\text{K}$ . Strong coupling between these two waves is to be expected on theoretical grounds<sup>1-4</sup> in the crossover region of the two dispersion curves, where the phase velocities are equal. This coupling was first demonstrated experimentally in potassium by Grimes and Buchsbaum.<sup>5</sup> With the parameters typical of  $n$ -PbTe at  $4.2^\circ\text{K}$  (electron concentration  $n \sim 10^{18} \text{ cm}^{-3}$ , mobility  $\mu \sim 10^{-6} \text{ cm}^2/\text{V sec}$ ), the coupling region can be reached with  $\mu B > 10$  ( $B$  = magnetic field strength) in the frequency range 500-1000 kHz.

In the present experiment, a resonant system was used (see Fig. 1) comprising two  $\lambda/2$  quartz transducers attached to the surfaces of a thin PbTe sample which also exhibited a  $\lambda/2$  acoustic resonance at the same frequency, and two crossed coils wound directly around the sample for excitation and detection of helicons. By applying a suitable magnetic field  $B$ , the helicon resonance frequency was tuned to the fixed acoustical resonance frequency.

With this arrangement, three types of experiments have been performed: (i) Phonon-phonon transmission (signal input, transducer 1; signal output, transducer 2). Fig. 1 shows the acoustic frequency response of the total system. (ii) Helicon-helicon transmission (input, coil 1; output, coil 2). (iii) Helicon-phonon transmission (input, coil 1; output, one transducer). The generation of phonons due to helicon excitation is shown by curve  $b$  of Fig. 1. In the third experiment, the second coil was used to monitor the input power so as to keep constant the helicon resonance amplitude within the sample. It should be noted from Fig. 1 that there is a slight difference of about 0.5% between the frequency of maximum phonon-phonon transmission and maximum helicon-phonon transmission. Whether this splitting is due to a deformation of the dispersion curves near the crossover point cannot be unambiguously decided at present.

By these experiments, we have demonstrated bulk generation of ultrasound by helicon waves clearly distinguished from the direct electromagnetic excitation (DEE) at the surface of the samples as reported previously.<sup>6,7</sup> This is supported by the following observations.

(a) In contrast to DEE, which leads to a linear increase of the sound amplitude with the static magnetic field,<sup>8</sup> the point of maximum helicon-phonon coupling is always given by  $v_{\text{phonon}} = v_{\text{helicon}}$ , i.e., at the simultaneous  $\lambda/2$  resonance of the helicon wave and the sound wave, as shown in Fig. 2. Here the helicon-helicon and the helicon-phonon transmission curves, taken at the (fixed) frequency of maximum helicon-phonon transmission, are plotted as a function of the magnetic field strength. The parameter in Fig. 2 is the angle  $\varphi$  between the magnetic field direction and the wave vector  $\vec{k}$  of the helicon wave. The magnetic field of maximum phonon excitation coincides for all angles up to  $67.5^\circ$  with the helicon resonance field. The angular dependence of the latter, which under isotropic conditions would be  $B_T^{-1} \sim \cos\varphi$ , shows in PbTe a slight anisotropy which has been studied both theoretically and exper-

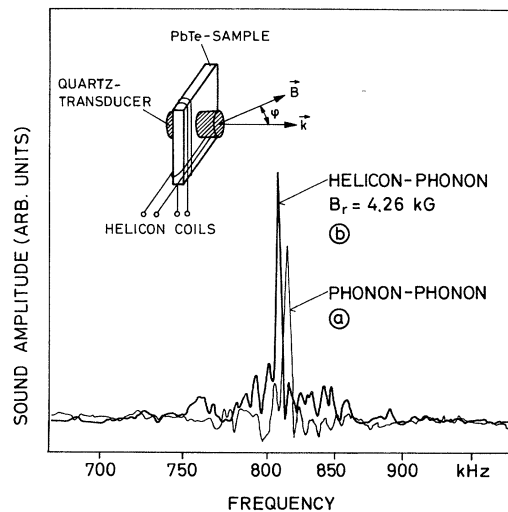


FIG. 1. Frequency response of the acoustic transmission (curve  $a$ ) and the helicon-phonon transmission (curve  $b$ : signal input, one helicon coil; signal output, one transducer) of the resonant system.

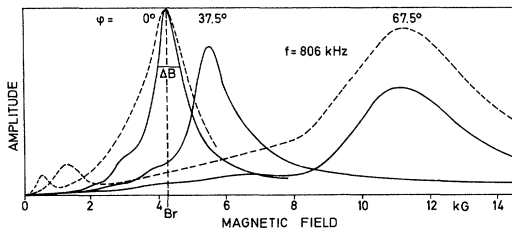


FIG. 2. Amplitude of the helicon-phonon transmission (solid curves) and helicon resonance curves (broken curves) versus magnetic field strength at various angles  $\phi$  between the directions of the magnetic field and the helicon wave vector.

imentally.<sup>9</sup>

(b) In addition to the fundamental  $\lambda/2$  resonance at  $B = B_{\gamma}$ , the helicon resonance curves exhibit  $3\lambda/2$  resonances at  $B \approx B_{\gamma}/9$  (the broken curves in Fig. 2). Although we have at this point simultaneous helicon and phonon resonance at the same frequency, there is no corresponding peak in the phonon amplitude curve, which clearly demonstrates that the coupling is very weak. This is just what is expected for bulk helicon-phonon coupling, because with this magnetic field the helicon velocity is only  $\frac{1}{3}$  of the phonon velocity, and the momentum mismatch prevents phonons from being generated.

(c) The peaks in the helicon-phonon transmission curves are always narrower than the helicon resonance curves, as shown, e.g., in Fig. 2, the ratio of the half widths being about 0.70 for  $\phi$  values up to  $50^\circ$ . The narrowing of the helicon-phonon transmission curve is presumed to be caused by the magnetic field dependence of the helicon-phonon coupling which is maximum at the crossing point  $B = B_{\gamma}$ .

In contrast to previous work which concerned only transverse sound waves, the results discussed above have been obtained for both longitudinal and transverse sound waves in samples of various crystallographic orientation and carrier concentration.<sup>10</sup> Strong differences occur in the angular dependence of the amplitude of the longitudinal and transverse sound waves. In Fig. 3 the maximum amplitudes of the two acoustic modes, measured at constant helicon resonance amplitude, are plotted (in arbitrary units) as a function of the angle  $\phi$ . In these measurements the wave vector was parallel to the  $\langle 111 \rangle$  crystal axis. Samples of

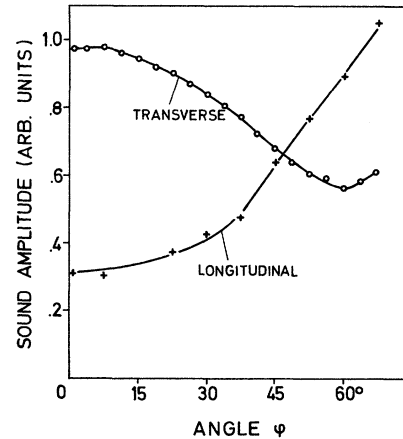


FIG. 3. Maximum amplitude of the transverse and longitudinal sound waves generated by helicon coupling versus angle  $\phi$  between magnetic field direction and helicon wave vector, measured at constant helicon resonance amplitude.

other crystallographic orientation and carrier concentration show qualitatively similar results which will be dealt with in detail in a forthcoming paper.

The author is indebted to Dr. C. A. A. J. Greebe, K. H. Sarges, Dr. K. J. Schmidt-Tiedemann, and Dr. K. Walther for helpful comments, and to K. Teschner for technical assistance.

<sup>1</sup>D. N. Langenberg and J. Bok, Phys. Rev. Letters **11**, 549 (1963).

<sup>2</sup>M. E. Browne, Helv. Phys. Acta **37**, 545 (1964).

<sup>3</sup>J. J. Quinn and S. Rodriguez, Phys. Rev. **133**, A1589 (1964).

<sup>4</sup>P. R. Antoniewicz and S. Rodriguez, J. Phys. Soc. Japan Suppl. **21**, 723 (1966).

<sup>5</sup>C. C. Grimes and S. J. Buchsbaum, Phys. Rev. Letters **12**, 357 (1964).

<sup>6</sup>J. R. Houck, H. V. Bohm, B. W. Maxfield, and J. W. Wilkins, Phys. Rev. Letters **19**, 224 (1967).

<sup>7</sup>K. Saermark and P. K. Larsen, Phys. Letters **24A**, 668 (1967).

<sup>8</sup>Deviations from the linear increase in PbTe samples were reported by Houck et al. (Ref. 6) and tentatively interpreted qualitatively by assuming acoustic generation throughout the bulk of the sample.

<sup>9</sup>W. Schilz, to be published.

<sup>10</sup>Coupling of helicon waves to both longitudinal and transverse sound waves at oblique magnetic fields in metals has been predicted theoretically by V. G. Skobov and E. A. Kaner, Zh. Eksperim. i Theor. Fiz. **46**, 273 (1964) [translation: Soviet Phys.-JETP **19**, 189 (1964)].